ACS APPLIED MATERIALS & INTERFACES

Forum Article

Cite This: ACS Appl. Mater. Interfaces 2019, 11, 2632−2637

www.acsami.org

Synthesis of Ultrathin Graphdiyne Film Using a Surface Template

Jingyuan Zhou,[†,‡] Ziqian Xie,[†] Rong Liu,[†,‡] Xin Gao,[†] Jiaqiang Li,[†,§] Yan Xiong,[§] Lianming Tong,[†] Jin Zhang,[*,†] and Zhongfan Liu[*,†]

[†]Center for Nanochemistry, Beijing Science and Engineering Center for Nanocarbons, Beijing National Laboratory for Molecular Sciences, College of Chemistry and Molecular Engineering, Peking University, Beijing 100871, P.R. China

[‡]Academy for Advanced Interdisciplinary Studies, Peking University, Beijing 100871, P.R. China

[§]School of Chemistry and Chemical Engineering, Chongqing University, Chongqing 401331, P.R. China

Supporting Information

ABSTRACT: Graphdiyne is predicted to have a natural band gap and simultaneously possesses superior carrier mobility, which makes it potential for electronic devices. Synthesis of ultrathin graphdiyne film is highly demanded. In this work, we proposed an approach for synthesis of ultrathin graphdiyne film using graphene as a surface template, which can induce confined reaction on substrate. With all-carbon, conjugated, atomically flat structure, graphene has a strong interaction with the graphdiyne system, resulting the formation of continuous flat ultrathin graphdiyne film with thickness less than 3 nm. Raman spectra, grazing incidence X-ray diffraction, and transmission electron microscopy characterization all confirmed the features of graphdiyne. Furthermore, this strategy was also extended to the hexagonal boron nitride (hBN) surface with resembling structure, serving as a perfect dielectric layer. Field-effect transistor devices based on graphdiyne film grown on hBN were fabricated directly, and electrical transport measurements demonstrate the good conductivity with *p*-type characteristics of the as-obtained graphdiyne film.

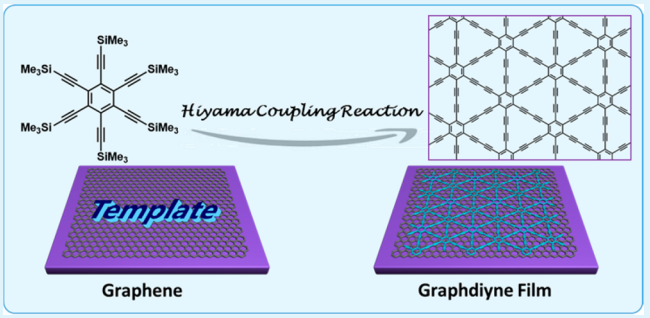

KEYWORDS: *graphdiyne, surface template, ultrathin film, graphene, hexagonal boron nitride (hBN)*

INTRODUCTION

Graphdiyne is a rapidly rising star of the carbon allotrope family. It refers to a two-dimensional structure with benzene rings connected by diyne linkages. The heat of formation of graphdiyne is predicted to be 18.3 kcal per g-atom C, which makes graphdiyne to be the most stable carbon allotrope containing diacetylenic linkages.[1] Theoretical calculation predicted that graphdiyne possesses natural moderate band gap of 0.46 eV and carrier mobility as high as 10^4 to 10^5 cm^2 V^{-1} s^{-1} at room temperature along with highly conjugated structure and uniformly distributed topological pores.[2] As a result of these prominent properties, graphdiyne has shown great potential in extensive applications such as Li-ion batteries,[3] photocatalysis,[4] solar cells,[5] photoelectrochemical water splitting cells (PEC),[6] oil/water separation,[7] etc. The intriguing electronic properties of bandgap along with simultaneous high mobility make graphdiyne an ideal candidate for all-carbon electronic circuits, overcoming the absence of band gap of graphene. From this aspect, synthesis of graphdiyne as continuous ultrathin film capable of in-plane charge transport is highly demanded for fabrication of integrated electronic devices used in practical applications. In 2010, graphdiyne film with thickness of 1 μm was synthesized successfully by using copper foil as both catalyst and substrate.[8] However, synthesis of continuous ultrathin graphdiyne film is still in infancy. The synthesis process goes through a troublesome problem of the free rotation of the alkyne-aryl single bonds, which leads to the coexistence of coplanar and twisted frameworks. For this purpose, we proposed a template synthesis method for confined reaction which would be beneficial for synthesis of ultrathin graphdiyne film.

Template synthesis is an effective method for synthesis of 2D layered materials. As we know, the interface molecular orientation is highly sensitive to the natural character of substrate, the essence of which is that the competition between the molecule interface and intermolecular interactions plays a decisive role in the molecular assembly manners.[9] Graphene, a single layer of sp^2 bonded carbon film with highly conjugated structure, is definitely an ideal choice as template for synthesis of ultrathin graphdiyne film. It has been reported as a good template for both organic and inorganic materials as well as conjugated molecular assembly. For example, covalent organic frameworks (COFs) grow as layers stacked horizontally to the

Special Issue: Graphdiyne Materials: Preparation, Structure, and Function

Received: February 12, 2018
Accepted: March 29, 2018
Published: April 5, 2018

DOI: 10.1021/acsami.8b02612
ACS Appl. Mater. Interfaces 2019, 11, 2632−2637

graphene surface, showing improved crystallinity compared with that of COFs powders.[10,11] Au nanoparticles are also found to grow on graphene surface with aligned array through a self-assembly process in solution because of the unique $\pi-\pi$ interaction.[12] Various conjugated organic molecules are favored to epitaxially grow with orientation on the surface of graphene induced severely by the strong graphene−molecule interaction.[13] For the purpose of preparing graphdiyne, a flat 2D film with all-carbon highly conjugated structure, graphene would naturally serve as a matched template.

Herein, we report a feasible synthetic route of ultrathin graphdiyne film by employing graphene as a substrate template, and graphdiyne film was found to grow selectively on the surface of graphene. Previously, Glaser coupling[8] and Glaser−Hay coupling[14] reactions were utilized for graphdiyne synthesis. In these reactions, monomer hexaethynylbenzene (HEB) was used for coupling reaction after deprotection of hexakis-[(trimethylsilyl)ethynyl]benzene (HEB-TMS) and protected by noble gas. However, there still would be slight amount of oxidation and self-polymerization side-reactions in the long reaction period. Therefore, we prefer to choose a reaction which could proceed with HEB-TMS monomer directly without deprotection. Hiyama reported that alkynylsilanes would smoothly dimerize in the presence of copper(I) salt in polar solvent such as *N*,*N*-dimethyformamide (DMF) or dimethyl sulfoxide (DMSO) to give 1,3-conjugated diynes with extremely high yield.[15] So, we utilized Hiyama coupling reaction by employing single layer graphene as template, and a continuous flat ultrathin graphdiyne film was synthesized successfully. Then, the composition and structure of the as-grown graphdiyne film were investigated completely. This process also worked well on the surface of hexagonal boron nitride (hBN) with resembling surface structure, which is a good dielectric layer. In this way, graphdiyne-based electronic devices were fabricated after exchanging the template graphene with hBN, demonstrating good conductivity with *p*-type characteristic.

EXPERIMENTAL SECTION

Graphene/hBN Transfer. Graphene grown on Cu foil was first transferred onto the SiO_2/Si substrate because Cu foil could not bare the DMF solution. Graphene was transferred with the assistance of poly(methyl methacrylate) (PMMA). After spin-coating with PMMA and being baked at 150 °C for 5 min, the back side of Cu foil with graphene was exposed to O_2 plasma for 3 min to remove the redundant graphene because graphene was grown on both sides of the Cu foil. After that, 1 M $FeCl_3$ solution was used to etch the copper away, and the free-standing PMMA-supported graphene was washed with DI water several times. Then, we transferred the film to the target substrate. After dying, the PMMA was subsequently removed by hot acetone vapor. Finally, the transferred graphene was annealing in Ar/H_2 at 400 °C for 2 h to remove the residues. CVD grown hBN was transferred with the same procedure.

Synthesis of Graphdiyne Film. Typically, HEB-TMS and CuCl with equivalent ratio 1:1 were added to a cylindrical pressure vessel and suspended in a mixture solution of THF and DMF (v/v 1:20). The small amount of THF was used for increasing solubility of the monomer. After capping, the mixed solution was sonicated for 10 min, and the SiO_2/Si with graphene was immersed in solution. The sealed vessel was heated at 65 °C for 6 h followed by 70 °C for 24 h. After reaction, the sample was subsequently washed by DMF, 1 M HCl, and DI water.

Ultrasonication Exfoliation Process. Substrates with graphdiyne film were immersed into the solution of NMP/EtOH and ultrasonicated for 15−30 min, forming stable dispersion.

Device Fabrication and Electronic Measurement. The electrodes were fabricated by standard photolithography procedure and thermal deposition of metal (8 nm Cr and 60 nm Au). The transport measurements were performed at room temperature using a Keithley 4200-SCS semiconductor characterization system, equipped with a four-probe station. During measurements, a 0.5 V DC bias was applied between source and drain with a linear sweep gate voltage from −50 to 50 V applied on back gate.

Characterizations. The as-grown graphdiyne film was analyzed by scanning electron microscopy (SEM, Hitachi S4800 field emission, acceleration voltage 2 kV), atomic force microscopy (AFM, Dimension Icon, Bruke Co.) in Scananalysis mode, transmission electron microscopy (TEM, FEI Tecnai F30, acceleration voltage 300 kV), and TEM (FEI Tecnai T20, acceleration voltage 120 kV) to investigate its morphology and structure. Raman spectrometry (Horiba HR800 Raman system) with laser excitation wavelength of 514.5 nm, X-ray photoelectron spectroscopy (XPS, ESCALab250, Thermo Scientific Corporation) was used to evaluate the composition of graphdiyne film on graphene. UV−vis spectra were recorded on a PerkinElmer Lambda 950 UV−vis spectrometer. Grazing incidence X-ray diffraction (GIXD) data was collected at beamline BL14B1 of Shanghai Synchrotron Radiation Facility (SSRF) at a wavelength of 1.2398 Å. BL14B1 is beamline based on bending magnet, and a Si(111) double crystal monochromator was employed to monochromatize the beam. The size of the focus spot is about 0.5 mm, and the end station is equipped with a Huber 5021 diffractometer. NaI scintillation detector was used for data collection.[16]

RESULTS AND DISCUSSION

The schematic illustration of the synthetic process is depicted in Figure 1a, and details are provided in the Supporting Information. Briefly, chemical vapor deposition (CVD) grown single layer graphene on Cu foil was transferred to SiO_2/Si substrate followed by thermal annealing. The substrate was immersed into the reaction solution. Under optimized solvothermal conditions with CuCl catalyst, a continuous flat graphdiyne film was obtained, covering the entire surface of graphene. A continuous ultrathin graphdiyne film grown on the surface of graphene could be identified from optical microscopy (OM) and SEM images in Figures 1b and c. The thinnest film

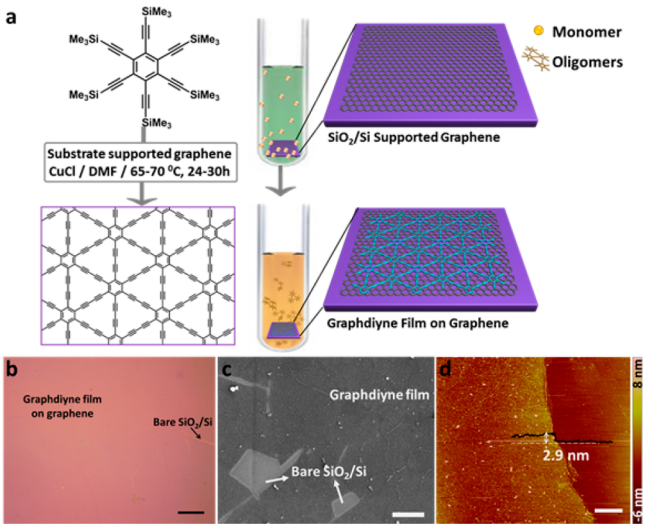

Figure 1. (a) Schematic presentation of the synthesis process of graphdiyne film grown on the surface of graphene. (b, c) Optical and SEM images of graphdiyne on graphene film on SiO_2/Si substrate. Scale bar, 20 and 5 μm, respectively. (d) Typical AFM image of graphdiyne on graphene. Scale bar, 5 μm.

DOI: 10.1021/acsami.8b02612
ACS Appl. Mater. Interfaces 2019, 11, 2632−2637

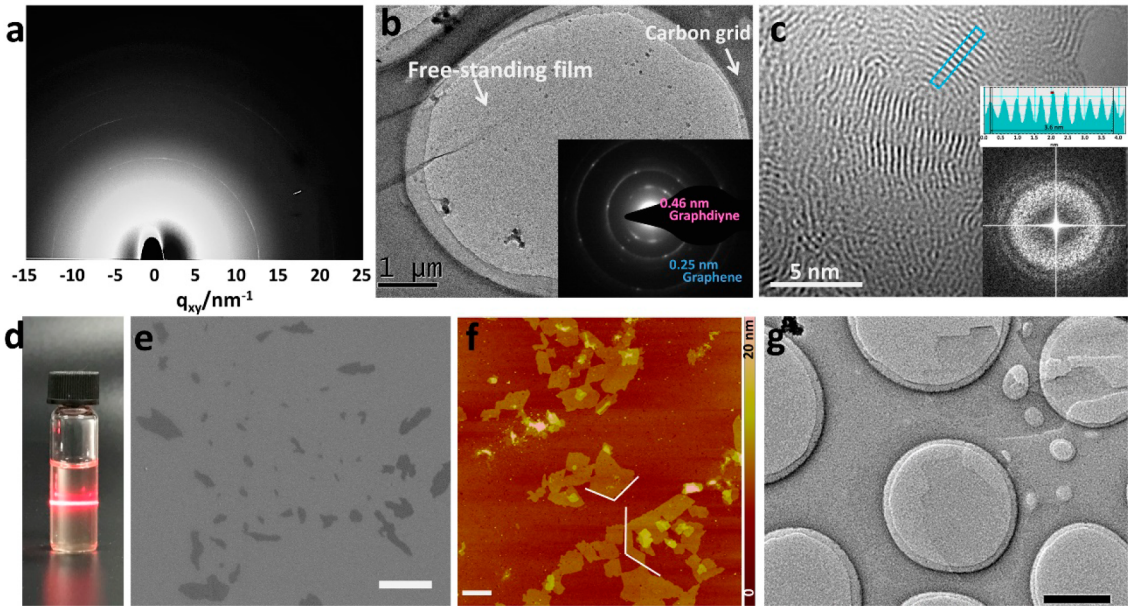

Figure 2. Structural characterization of graphdiyne film grown on graphene. (a) GIXD image collected for graphdiyne film showing presence of Bragg rings. (b) TEM image of transferred graphdiyne film on graphene. Corresponding SEAD pattern is in inset, and the patterns of graphdiyne and graphene are labeled, respectively. (c) HRTEM image of transferred graphdiyne film. Related FFT pattern is in the corresponding inset. Line profile at position along the blue square representing interlayer spacing of multilayer graphdiyne. (d) Photograph of graphdiyne nanosheets dispersion in NMP/EtOH solution showing an apparent Tyndall effect. (e, f) SEM and AFM images of graphdiyne nanosheets. Scale bar, 2 and 1 μm, respectively. (g) TEM image of dispersed nanosheets. Scale bar, 2 μm.

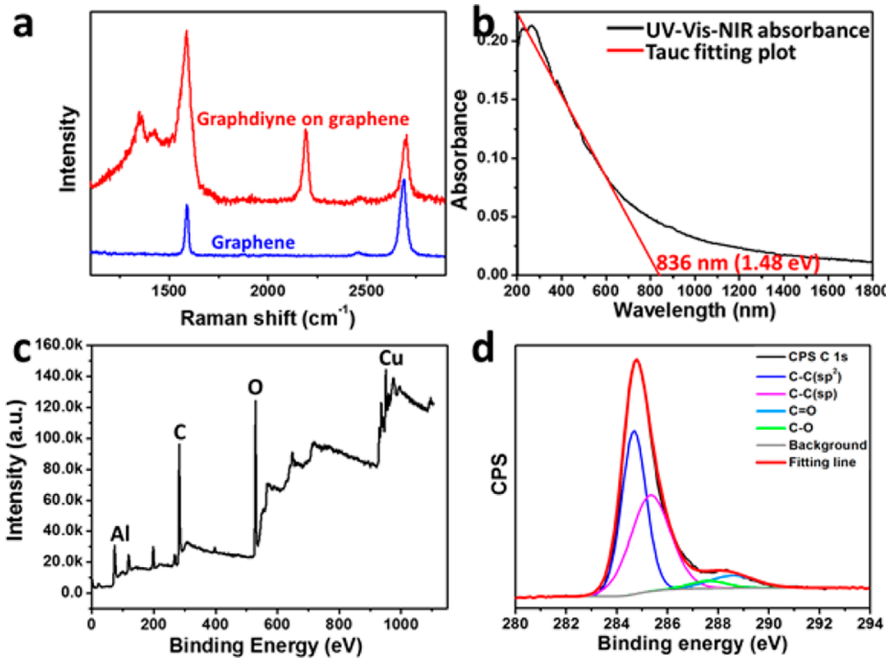

Figure 3. (a) Raman spectra evolution of graphene and as-grown graphdiyne on graphene. (b) UV−vis−NIR absorbance spectra. Tauc plot corresponds to optical band gap of 1.48 eV. (c) XPS spectra of graphdiyne film on Al_2O_3 substrate (survey scan). (d) XPS spectra of graphdiyne for C 1s.

was 2.9 nm according to AFM results in Figure 1d, and the thickness could also be tuned by concentration of monomer ranging from 3 to 20 nm.

As such a new material, we are extremely concerned with the structural characterization. In Figure 2a, the GIXD image collected for graphdiyne film demonstrates the presence of Brag rings at 12.9, 17.6, and 21.0 nm^{-1}, corresponding to *d*-spacing of 0.48, 0.36, and 0.30 nm, respectively. The *d*-spacing of 0.48 and 0.30 nm correspond to (1,1,0) facet and (2, 1, 0) facet of graphdiyne, respectively. The 0.36 nm refers to the interlayer spacing, indicating that graphdiyne is a two-dimensional layered material. TEM was also employed for structural identification. As shown in Figure 2b, the as-grown graphdiyne film could be transferred to grid as a free-standing film by traditional transfer method with assistance of PMMA. The corresponding selected-area electron diffraction (SAED) patterns in Figure 2b show the

DOI: 10.1021/acsami.8b02612
ACS Appl. Mater. Interfaces 2019, 11, 2632−2637

patterns of graphene and graphdiyne at the same time. Referring to graphene with d = 0.25 nm, the first order diffraction of graphdiyne d = 0.47 nm refers to (1,1,0) lattice facet and its equivalent planes. This result matches quite well with that of graphdiyne with ABC stacking manner.[17,18] In high-resolution TEM (HRTEM) image in Figure 2c, it clearly reveals curved streaks with a lattice parameter of 0.36 nm, which corresponds to the π-stacking interlayer distance of two-dimensional layers. This result is also according to calculated interlayer spacing value ranging from 0.34 to 0.37 nm with different stacking configurations.[19] It hence appears that two-dimensional layered graphdiyne film with good crystallinity was obtained successfully.

Furthermore, inspired by liquid exfoliation of graphene,[20] graphdiyne dispersion was obtained by repeated ultrasonication of the film on substrate in NMP/EtOH solution. The graphdiyne dispersion gave rise to obvious Tyndall effect as a result of light scattering, indicating colloidal nature of the dispersion (Figure 2d). Some initial characterizations were executed by spin-coating the dispersion onto a SiO_2/Si substrate. SEM image was collected in Figure 2e showing some isolated nanosheets with lateral size of 0.5−3.0 μm. AFM image in Figure 2f shows that the resulting graphdiyne sheets are flat with thickness of 3−4 nm. The corners remain sharp, and the edges are well-defined. TEM sample was prepared by pipetting the dispersion onto the grid, and the TEM image in Figure 2g illustrates the uniformly dispersed nanosheets with nearly transparent feature inferred their ultrathin thickness with good crystallinity. The simple process of exfoliation sufficiently demonstrated the layered characteristic of graphdiyne.

Bonding structure and elementary composition of the graphdiyne film on graphene was investigated systemically. Prominently, Raman spectroscopy has historically played an important role in the study and characterization of carbon material and it is also a competent technique for investigation of Raman-active C−C triple bond.[21] The Raman spectra of graphdiyne film grown on graphene is shown in Figure 3a. The peak around G peak position is not symmetric and can be deconvoluted into two peaks at 1540 and 1586 cm^{-1} attributed to the G peaks of graphdiyne film and graphene substrate, respectively. The peaks at 1586 and 2700 cm^{-1} are the typical G and 2D peaks of graphene. Comparison between before and after reaction shows upshift of graphene Raman peak because of doping effect.[22,23] As for graphdiyne, the peak at 1350 cm^{-1} is ascribed to the scissoring vibration of atoms in benzene.[24] 1421 cm^{-1} peak refers to the vibrations of C−C bonds between triply coordinated atoms and their doubly coordinated neighbors. The G peak at 1540 cm^{-1} mostly comes from in-phase stretching of aromatic bonds common in all sp^2 carbon system. Yet, the wavenumber of the G peak is relatively lower in alkyne-rich material, which reflects the influence of conjugated effects.[25] The peak at 2190 cm^{-1} corresponds to the stretching mode of diacetylene bond. Remarkably, compared with reported results, the diyne peak displays much higher intensity and less half-peak breadth.[8,14] Briefly, the Raman spectra is in good agreement with theoretical result, indicating the formation of proposed structure. Meanwhile, the spectra of XPS in Figure 3c indicates that graphdiyne film is primarily composed of elemental carbon, which is coincident with the result of EDS in Figure S5. In Figure 3d, the deconvolution of C 1s peak resolved four subpeaks, corresponding to C−C (sp^2) at 284.5 eV, C−C (sp) at 285.4 eV, C−O at 287.5 eV, and C═O at 288.6, respectively.[26] To investigate the optical properties of as-prepared graphdiyne film, UV−vis−NIR absorption spectrum was carried out. For in situ growth on quartz, graphene was first transferred onto optical grade quartz followed by standard graphdiyne film growth procedure, and the background was subtracted using a blank quartz with a layer of graphene. On the basis of Tauc's formulation, extension cord of the linear section and λ-axis would make an intersection point, representing the optical band gap.[27,28] As shown in Figure 3b, it is speculated that the optical band gap of graphdiyne film is 1.48 eV. The optical band gap is a little larger than the calculated result, and the rational explanations are calculated deviation, p-doping effect, excessive defects, and spatial confinement of the limited grain size in the film. All these structural and spectroscopic characterizations are in good agreement with the theoretical model, leading to the conclusion that we synthesized graphdiyne film which is consistent with the theoretical structure.[2]

It is remarkable that the graphdiyne film would prefer to grow on the surface of graphene rather than on SiO_2/Si. The selective growth could be characterized by Raman mapping. Graphene was first patterned with an array of circles by photolithography, and Figure 4a presents the corresponding optical image. After reaction, Raman mapping was performed with 2D peak of graphene at 2700 cm^{-1} and diyne peak of graphdiyne at 2190 cm^{-1} (Figure 4b). The results profile that the shape of graphdiyne was exactly consistent with that of graphene, which further solidifies the facilitation of graphene for the growth of graphdiyne film.

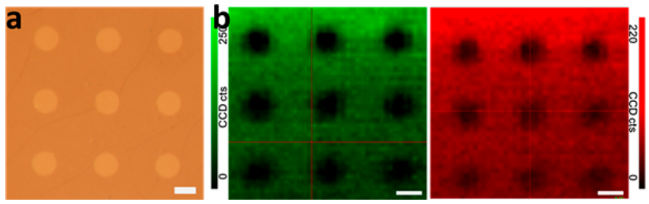

Figure 4. (a) Optical image of pattern graphene fabricated by photolithography. Scale bar, 5 μm. (b) Left: 2D band mapping of graphene. Right: diyne peak mapping of graphdiyne, revealing that graphdiyne film is selectively grown on the surface of graphene. Scale bar, 5 μm.

Taking into account the excellent conductivity of graphene itself, we replace graphene with CVD grown hBN for electric measurement. hBN is an excellent layered insulator material with a wide direct band gap of 5.9 eV and could be a reliable dielectric layer in electronic devices. It structurally resembles graphene and was also proved to be beneficial for aromatic molecule self-assemble and COFs (covalent organic frameworks) film growth.[29,30] Therefore, we extended this template method to hBN, and the same synthesis process was executed with hBN as surface template instead of graphene. The graphdiyne film grown on hBN shows similar Raman feature to that grown on graphene (Figure. S6). The sharp diyne peak is an indication of graphdiyne film.

Fundamental transport measurements were performed to estimate the electronic properties of the ultrathin graphdiyne film. A schematic depiction of the device is shown in Figure 5a. Typical I−V characteristic is shown in Figure 5b, displaying good conductivity of graphdiyne film, and the linear behavior indicates ohmic-like contact between the sample and electrodes. Figures 5c and d show the output and transfer characteristics of the device. When the V_g is positive scanning

DOI: 10.1021/acsami.8b02612
ACS Appl. Mater. Interfaces 2019, 11, 2632−2637

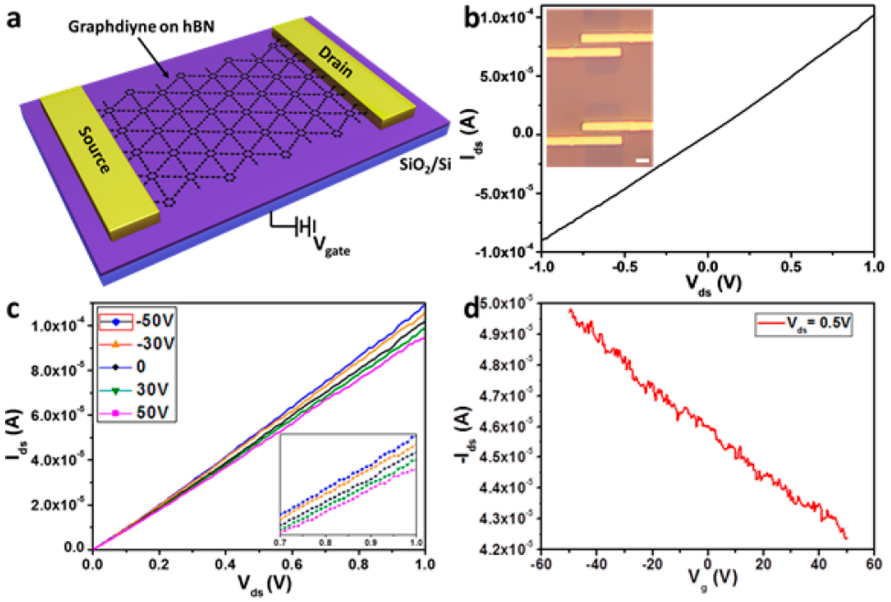

Figure 5. Electrical properties of graphdiyne film. (a) Three-dimensional schematic view of graphdiyne transistor. (b) $I-V_{ds}$ characteristic for the device. Inset: OM image of the device. Scale bar, 5 μm. (c) $I_{ds}-V_{ds}$ curves recorded under various V_g biases from −50 to 50 V. (d) Transport characteristic curve of the device at V_{ds} = 0.5 V.

the conductance decreases, showing a p-type semiconducting characteristic. The field-effect mobility of graphdiyne film grown on hBN is calculated as 6.25 $cm^2\ V^{-1}\ s^{-1}$ using the equation $\mu = [dI/dV_g][L/(WC_gV_{ds})]$, where L = 2 μm, W = 5 μm, and C_g = 12.1 $nF{\cdot}cm^{-2}$ ($C_g = \varepsilon_r\varepsilon_0/d$, d = 285 nm).[31]

The conductivity of the graphdiyne film originated from its extensive conjugated sp^2 and sp carbon networks. It is notable that this value is among the top level of organic field-effect transistor (OFET) or COF-based devices because of the integrated conjugated covalent bonding in planar network. In addition, different 2D templates were also compared and are discussed in the Supporting Information, and Figure S7 shows corresponding results. It can be deduced that the graphdiyne films grown on graphene and hBN are of higher quality, indicating that a graphene-like 2D atomic flat surface template, which can increase the interaction between graphdiyne system and substrate surface, is essential for growth of high quality ultrathin graphdiyne film. The FET mobility is far lower than that of the theoretical result because the carrier mobility of graphdiyne is considerably more sensitive to defects and domain boundaries, which interrupts conjugation and increases phonon scattering. We are still on the way to further optimizing for larger planar domains with fewer defects and extending potential applications of graphdiyne in electronics.

CONCLUSION

In summary, continuous flat ultrathin graphdiyne film was synthesized successfully by employing graphene as a template, which would increase the interaction between the graphdiyne system and substrate surface. The as-grown graphdiyne film could also be exfoliated in solution, forming stable dispersion. Systematic characterization confirmed the composition and structure of the film. Meanwhile, graphdiyne-based FET devices were also fabricated after extending this template strategy to hBN, which demonstrated good conductivity and *p*-type characteristic. This template method promoted the formation of ultrathin graphdiyne film and provided a step forward for the broad prospect of its applications in electronic devices. We also paved a considerably feasible way for further exploring the fundamental properties of graphdiyne.

ASSOCIATED CONTENT

Supporting Information

The Supporting Information is available free of charge on the ACS Publications website at DOI: 10.1021/acsami.8b02612.

Experimental details, survey scan of XPS, EDS analysis of the graphdiyne film, graphdiyne film grown on hBN surface, and comparison of different substrates (PDF)

AUTHOR INFORMATION

Corresponding Authors

*E-mail: jinzhang@pku.edu.cn.
*E-mail: zfliu@pku.edu.cn.

ORCID

Yan Xiong: 0000-0002-5258-5325
Lianming Tong: 0000-0001-7771-4077
Jin Zhang: 0000-0003-3731-8859
Zhongfan Liu: 0000-0003-0065-7988

Funding

This work was supported by the Ministry of Science and Technology of China (Grants 2016YFA0200101 and 2016YFA0200104), National Natural Science Foundation of China (Grants 51432002, 51720105003, and 21790052), and Beijing Municipal Science and Technology Project (Project 161100002116026).

Notes

The authors declare no competing financial interest.

ACKNOWLEDGMENTS

The authors thank Bangjun Ma for guidance on device fabrication, Li Lin and Qiucheng Li for CVD growth of graphene and hBN, and Zhenzhu Li and Jinying Wang for valuable discussion from the perspective of theoretical calculation. The authors thank beamline BL14B1 (Shanghai

DOI: 10.1021/acsami.8b02612
ACS Appl. Mater. Interfaces 2019, 11, 2632−2637

Synchrotron Radiation Facility) for providing the beam time and help during experiments.

REFERENCES

(1) Haley, M. M.; Brand, S. C.; Pak, J. J. Carbon Networks Based on Dehydrobenzoannulenes: Synthesis of Graphdiyne Substructures. *Angew. Chem., Int. Ed. Engl.* **1997**, *36*, 836−838.
(2) Long, M.; Tang, L.; Wang, D.; Li, Y.; Shuai, Z. Electronic Structure and Carrier Mobility in Graphdiyne Sheet and Nanoribbons: Theoretical Predictions. *ACS Nano* **2011**, *5*, 2593−2600.
(3) Huang, C.; Zhang, S.; Liu, H.; Li, Y.; Cui, G.; Li, Y. Graphdiyne for high capacity and long-life lithium storage. *Nano Energy* **2015**, *11*, 481−489.
(4) Yang, N.; Liu, Y.; Wen, H.; Tang, Z.; Zhao, H.; Li, Y.; Wang, D. Photocatalytic Properties of Graphdiyne and Graphene Modified TiO_2: From Theory to Experiment. *ACS Nano* **2013**, *7*, 1504−1512.
(5) Kuang, C.; Tang, G.; Jiu, T.; Yang, H.; Liu, H.; Li, B.; Luo, W.; Li, X.; Zhang, W.; Lu, F.; Fang, J.; Li, Y. Highly Efficient Electron Transport Obtained by Doping PCBM with Graphdiyne in Planar-Heterojunction Perovskite Solar Cells. *Nano Lett.* **2015**, *15*, 2756−2762.
(6) Li, J.; Gao, X.; Liu, B.; Feng, Q.; Li, X.-B.; Huang, M.-Y.; Liu, Z.; Zhang, J.; Tung, C.-H.; Wu, L.-Z. Graphdiyne: A Metal-Free Material as Hole Transfer Layer To Fabricate Quantum Dot-Sensitized Photocathodes for Hydrogen Production. *J. Am. Chem. Soc.* **2016**, *138*, 3954−3957.
(7) Gao, X.; Zhou, J.; Du, R.; Xie, Z.; Deng, S.; Liu, R.; Liu, Z.; Zhang, J. Robust Superhydrophobic Foam: A Graphdiyne-Based Hierarchical Architecture for Oil/Water Separation. *Adv. Mater.* **2016**, *28*, 168−173.
(8) Li, G.; Li, Y.; Liu, H.; Guo, Y.; Li, Y.; Zhu, D. Architecture of graphdiyne nanoscale films. *Chem. Commun.* **2010**, *46*, 3256−3258.
(9) Giri, G.; Verploegen, E.; Mannsfeld, S. C. B.; Atahan-Evrenk, S.; Kim, D. H.; Lee, S. Y.; Becerril, H. A.; Aspuru-Guzik, A.; Toney, M. F.; Bao, Z. Tuning charge transport in solution-sheared organic semiconductors using lattice strain. *Nature* **2011**, *480*, 504−508.
(10) Colson, J. W.; Woll, A. R.; Mukherjee, A.; Levendorf, M. P.; Spitler, E. L.; Shields, V. B.; Spencer, M. G.; Park, J.; Dichtel, W. R. Oriented 2D Covalent Organic Framework Thin Films on Single-Layer Graphene. *Science* **2011**, *332*, 228−231.
(11) Sun, B.; Zhu, C.-H.; Liu, Y.; Wang, C.; Wan, L.-J.; Wang, D. Oriented covalent organic framework film on graphene for robust ambipolar vertical organic field-effect transistor. *Chem. Mater.* **2017**, *29*, 4367−4374.
(12) Huang, X.; Li, S.; Huang, Y.; Wu, S.; Zhou, X.; Li, S.; Gan, C. L.; Boey, F.; Mirkin, C. A.; Zhang, H. Synthesis of hexagonal close-packed gold nanostructures. *Nat. Commun.* **2011**, *2*, 292.
(13) Kim, K.; Santos, E. J. G.; Lee, T. H.; Nishi, Y.; Bao, Z. Epitaxially Grown Strained Pentacene Thin Film on Graphene Membrane. *Small* **2015**, *11*, 2037−2043.
(14) Zhou, J.; Gao, X.; Liu, R.; Xie, Z.; Yang, J.; Zhang, S.; Zhang, G.; Liu, H.; Li, Y.; Zhang, J.; Liu, Z. Synthesis of Graphdiyne Nanowalls Using Acetylenic Coupling Reaction. *J. Am. Chem. Soc.* **2015**, *137*, 7596−7599.
(15) Ikegashira, K.; Nishihara, Y.; Hirabayashi, K.; Mori, A.; Hiyama, T. Copper(i) salt promoted homo-coupling reaction of organosilanes. *Chem. Commun.* **1997**, *11*, 1039−1040.
(16) Yang, T.; Wen, W.; Yin, G.; Li, X.; Gao, M.; Gu, Y.; Li, L.; Liu, Y.; Lin, H.; Zhang, X.; Zhao, B.; Liu, T.; Yang, Y.; Li, Z.; Zhou, X.; Gao, Z. Introduction of the X-ray diffraction beamline of SSRF. *Nucl. Sci. Technol.* **2015**, *26*, 20101.
(17) Li, C.; Lu, X.; Han, Y.; Tang, S.; Ding, Y.; Liu, R.; Bao, H.; Li, Y.; Luo, J.; Lu, T. Direct imaging and determination of the crystal structure of six-layered graphdiyne. *Nano Res.* **2018**, *11*, 1714−1721.
(18) Matsuoka, R.; Sakamoto, R.; Hoshiko, K.; Sasaki, S.; Masunaga, H.; Nagashio, K.; Nishihara, H. Crystalline Graphdiyne Nanosheets Produced at a Gas/Liquid or Liquid/Liquid Interface. *J. Am. Chem. Soc.* **2017**, *139*, 3145−3152.
(19) Zheng, Q.; Luo, G.; Liu, Q.; Quhe, R.; Zheng, J.; Tang, K.; Gao, Z.; Nagase, S.; Lu, J. Structural and electronic properties of bilayer and trilayer graphdiyne. *Nanoscale* **2012**, *4*, 3990−3996.
(20) Li, D.; Muller, M. B.; Gilje, S.; Kaner, R. B.; Wallace, G. G. Processable aqueous dispersions of graphene nanosheets. *Nat. Nanotechnol.* **2008**, *3*, 101−105.
(21) Dresselhaus, M. S.; Jorio, A.; Hofmann, M.; Dresselhaus, G.; Saito, R. Perspectives on Carbon Nanotubes and Graphene Raman Spectroscopy. *Nano Lett.* **2010**, *10*, 751−758.
(22) Bae, S.; Kim, H.; Lee, Y.; Xu, X.; Park, J.-S.; Zheng, Y.; Balakrishnan, J.; Lei, T.; Ri Kim, H.; Song, Y. I.; Kim, Y.-J.; Kim, K. S.; Ozyilmaz, B.; Ahn, J.-H.; Hong, B. H.; Iijima, S. Roll-to-roll production of 30-in. graphene films for transparent electrodes. *Nat. Nanotechnol.* **2010**, *5*, 574−578.
(23) Malard, L. M.; Pimenta, M. A.; Dresselhaus, G.; Dresselhaus, M. S. Raman spectroscopy in graphene. *Phys. Rep.* **2009**, *473*, 51−87.
(24) Wang, J.; Zhang, S.; Zhou, J.; Liu, R.; Du, R.; Xu, H.; Liu, Z.; Zhang, J.; Liu, Z. Identifying *sp-sp*^{2} carbon materials by Raman and infrared spectroscopies. *Phys. Chem. Chem. Phys.* **2014**, *16*, 11303−11309.
(25) Zhang, S.; Wang, J.; Li, Z.; Zhao, R.; Tong, L.; Liu, Z.; Zhang, J.; Liu, Z. Raman Spectra and Corresponding Strain Effects in Graphyne and Graphdiyne. *J. Phys. Chem. C* **2016**, *120*, 10605−10613.
(26) Ihm, K.; Kang, T.-H.; Lee, D. H.; Park, S.-Y.; Kim, K.-J.; Kim, B.; Yang, J. H.; Park, C. Y. Oxygen contaminants affecting on the electronic structures of the carbon nano tubes grown by rapid thermal chemical vapor deposition. *Surf. Sci.* **2006**, *600*, 3729−3733.
(27) Tauc, J.; Grigorovici, R.; Vancu, A. Optical Properties and Electronic Structure of Amorphous Germanium. *Phys. Status Solidi B* **1966**, *15*, 627−637.
(28) Behura, S.; Nguyen, P.; Che, S.; Debbarma, R.; Berry, V. Large-area, transfer-free, oxide-assisted synthesis of hexagonal boron nitride films and their heterostructures with MoS2 and WS_2. *J. Am. Chem. Soc.* **2015**, *137*, 13060−13065.
(29) Zhang, Y.; Qiao, J.; Gao, S.; Hu, F.; He, D.; Wu, B.; Yang, Z.; Xu, B.; Li, Y.; Shi, Y.; Ji, W.; Wang, P.; Wang, X.; Xiao, M.; Xu, H.; Xu, J.-B.; Wang, X. Probing Carrier Transport and Structure-Property Relationship of Highly Ordered Organic Semiconductors at the Two-Dimensional Limit. *Phys. Rev. Lett.* **2016**, *116*, 016602.
(30) Medina, D. D.; Sick, T.; Bein, T. Photoactive and Conducting Covalent Organic Frameworks. *Adv. Energy Mater.* **2017**, *7*, 1700387.
(31) Radisavljevic, B.; Radenovic, A.; Brivio, J.; Giacometti, V.; Kis, A. Single-layer MoS_2 transistors. *Nat. Nanotechnol.* **2011**, *6* (3), 147−150.

DOI: 10.1021/acsami.8b02612
ACS Appl. Mater. Interfaces 2019, 11, 2632−2637